Michigan State University

National Superconducting Cyclotron Laboratory

SECONDARY DECAYS AND THE HELIUM LITHIUM ISOTOPE THERMOMETER

H. XI, W.G. LYNCH, M.B. TSANG, and W.A. FRIEDMAN

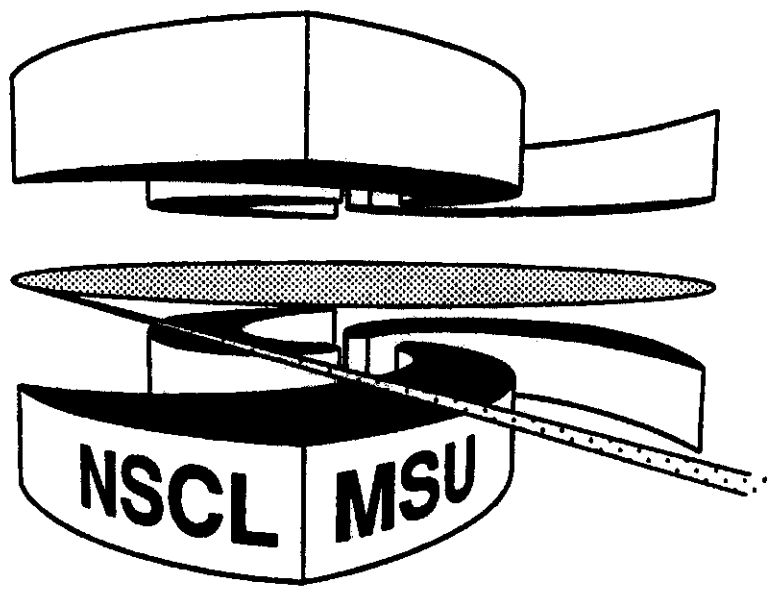

MSUCL-1040

AUGUST 1996

Secondary Decays and the Helium Lithium Isotope Thermometer

H. Xi, W.G. Lynch, M.B. Tsang,

National Superconducting *Cyclotron Laboratory* and *Deportment of Physics and Astronomy, Michigan State University, East Lansing, MI 48824, USA,*

W.A. Friedman,

Department of Physics, University of Wisconsin, Madison, WI 53706, USA

(August 23, 1996)

Abstract

Detailed sequential decay calculations which include both discrete states and unbound states in the continuum have been performed. Particular attention is paid to the lifetime of continuum states contributing to the process and to the role of the primary charge distribution. Comparisons to the recent data indicate that determination of temperatures greater than 7 MeV is problematic due to sequential feedings from continuum states and uncertainties in the primary charge distribution prior to secondary decay.

Recently analyses of isotopic yields for multifragment decays of $Au + Au$ collisions at $E/A = 600$ MeV yield temperatures that remain relatively constant as a function of deduced excitation energy for 2.5 MeV$\leq E^*/A \leq$ 10 MeV but increase rapidly at $E^*/A \geq 10$ MeV [1]. The similarity of these observations to the predictions of microcanonical models[2,3] for nuclear multifragmentation have stimulated investigations[4-9] aimed at addressing whether such observables provide significantly new information about the liquid gas phase transition of nuclear matter.

The evidence of the rapid increase in the temperature at $E^*/A \geq 10$ MeV reported in ref. [1] relies primarily upon the extraction of temperature from the expression [1, 8]

$$T_{HeLi} = C\frac{13.32}{\ln(2.18R_{HeLi})} \tag{1}$$

where $R_{HeLi} = \{Y(^6Li)/Y(^7Li)\}/\{Y(^3He)/Y(^4He)\}$, $Y(X)$ is the yield for isotope X and C is a constant which assumes the value, $C = 1$, in the ideal case that $Y(X)$ are the ground state yields consistent with global thermal and chemical equilibrium. However, the observed populations of isotopes are influenced strongly by the sequential decay of heavier particle unstable nuclei which occurs after these nuclei leave the disintegrating system. In reference [1], C was set to 1.2 in an attempt to correct for such effects.

Apriori, it is not clear that a constant multiplicative overall renormalization of Eq. 1 as proposed by ref. [1] provides a reasonable accounting for sequential decay corrections. Guidance for the constant renormalization factor of $C = 1.2$ was obtained by ref. [1] within the context of the Quantum Statistical Model (QSM) [10] (and other statistical models which do not include sequential decays); more recent QSM calculations suggest values for C ranging from 1.4 to 1.8 as the excitation energy is varied over the range $E^*/A = 2.5$ MeV to 15 MeV [9]. Both investigations with the QSM model, however, considered only the decays from tabulated discrete states [1,9,10]. Other important decay pathways which pass through continuum states and through discrete states that have not been experimentally characterized are neglected therein. To achieve an accurate description of secondary decay effects [12-14], these states must be counted in accordance with empirical level density

information [11]]. Decays from continuum states have been included in calculations which successfully describe the measured isotope ratios and excited state populations for central $^{36}Ar + ^{197}Au$ collisions at 35 AMeV[4]. Here we reanalyze the "caloric curve" data of ref. [1] using an approach similar to that in ref. [4,12-13] in order to address the role of secondary decay from both discrete states and unbound states.

To address questions relating to the emission temperature, we allow the emission of nuclei with $1 \leq Z \leq 20$ in their ground states or in any of their excited states. The spectrum of allowed excited states includes both the known and tabulated [15] excited states as well as an empirically based extrapolation of the level density into the continuum as described in ref. [12,14]. We approximate the emission by two stages: 1) a first stage where these states are initially populated when the fragments are emitted from the system, and 2) a second stage during which the excited fragments decay according to standard statistical theory. Understanding the influence of this second stage of the decay process upon the isotope temperatures of ref. [1] is the major focus of this investigation.

We assume that the first stage of emission can be described by statistical decay mechanisms; possible candidates range from the evaporation from a heavy residue to the complete vaporization of the system. For simplicity, we approximate the initial population of an excited state of an emitted nucleus with excitation energy E_i^*, spin J_i , neutron number N_i and charge number Z_i with the expression

$$P_i(N_i\ ,\ Z_i\ ,\ E_i^*,\ \mu_p,\ \mu_n,\ T_{em})_\propto$$
$$(2J_i+1)\cdot(N_i+Z_i)^{1.5}\exp(-\tfrac{V_i}{T_{em}}+\tfrac{Q_i}{T_{em}})\exp(-\tfrac{E_i^*}{T_{em}})\exp(-\tfrac{Z_i\mu_p+N_i\mu_n}{T_{em}})\exp(-t_b/t_i), \quad (2)$$

where V_i is the Coulomb barrier, $-Q_i$ is the separation energy for emission of this nucleus from a residue of mass number A_o and charge number Z_o, T_{em} is the emission temperature and $\exp(-t_b/t_i)$ is a factor which suppresses the emission of very short-lived nuclei. Values for A_o at the deduced excitation energy $< E_o/A_o > for$ each data point in Table I were taken from ref. [1] and Z_o was obtained from A_o by requiring the projectile-like prefragment to have the same charge to mass ratio as the projectile. The "chemical potentials", μ_p and

μ_n, were treated as free parameters to reproduce the experimental charge distributions[16].

For the second (decay) stage of the calculation, we focus on the decay of nuclei from both tabulated low lying discrete states[15] and continuum states. Each decay was calculated using tabulated branching ratios where available[15] and the Hauser-Feshbach formalism [17], when such information is unavailable. Unknown spins and parities of tabulated discrete states were randomly assigned in these calculations [12,13] and then changed in subsequent calculations to assess the corresponding uncertainties. In general, the uncertainties in R_{HeLi} due to the uncertainties in the unknown spins and parities are of the order of 5%.

As the excitation energy is increased into the continuum, the calculations must consider decays of short-lived states with no barrier to particle emission; however, it is likely that many such short-lived states will decay before break up[18-20]. To take this pre-breakup cooling effect into account, we include in the initial population a factor, $\exp(-t_b/t_i)$. Here, $t_i = t(E^*/A)$ is the mean lifetime of the emitted fragment calculated according to the Weisskopf model [21,22] for statistical decay; t_b is the breakup timescale chosen to be 100 fm/c for this model study. To shorten computation times, an additional constraint $E_i^*/A_o \leq 5MeV$ was imposed on the continuum. The influence of this constraint, discussed in greater detail below, is limited to the highest initial temperatures with $T_{em} > 7$ MeV.

Calculations were performed as a function of the emission temperature T_{em} to reproduce the representative experimental data given in Table 1; these data span the range of excitation energies investigated in ref. [1]. The corresponding experimental charge distributions were parameterized by a power law distributions $Y(Z) \propto Z^{-\tau}$ in ref. [23] with τ values given in the table. In our calculations, μ_p and μ_n were not apriori given the values assigned to them as "chemical potentials "[18, 24, 25] or "free excitation energies"[19] within specific statistical models. Instead, they were adjusted to reproduce the measured charge distributions subject to the constraint that the total charge to mass ratio of the emitted particles was consistent with the initial total charge to mass ratio Z_o/A_o[26]. Reproduction of the measured charge distributions is particularly important when the temperature is large and many excited states are populated since calculated charge distributions that are too steep (too shallow)

will underpredict (overpredict) the secondary feeding corrections. Indeed, for the sequential decay calculations $at < E_o/A_o >= 13.2$ and 15.1 MeV, changes in τ comparable to the experimental uncertainty $of \pm 0.5$, result in changes of 8-10% in R_{HeLi} for temperature greater than 5 MeV.

The solid lines in Figure 1 show the calculated double ratios R_{HeLi} as a function of the emission temperatures, T_{em} , for each data point listed in Table I. The corresponding values for the excitation energy from ref. [1] and τ from ref. [23] are labeled in each panel of Figure 1. The width of the calculated lines represents the aforementioned 5% uncertainty stemming from the unknown spins and parities of excited states feeding the Helium and Lithium isotopes and also the uncertainty due to the experimental uncertainty of τ. In all calculations, R_{HeLi} flatten out at high temperature, indicating that extremely precise experimental measurements and theoretical calculations would be needed to extract temperatures above $T_{em} > 7$ MeV. If the constraint $E_i^*/A_o \leq 5$ MeV is removed, the calculations become even flatter at $T_{em} > 7$ MeV, and the temperature range for agreement between calculations and data remains unchanged.

To illustrate this flattening is due to the decay from continuum states in sequential decay calculations, we repeated the calculations for the data $at < E_o/A_o >= 13.2$ MeV, $\tau = 2.5$ including only the discrete states. The results without continuum states, shown by the dashed lines in the second right panel of Figure 1, agree with the QSM calculations used in ref. [1], but fall below the calculations with the continuum states beyond $T_{em} = 6$ MeV.

We now turn to the comparison of our calculations to the data of ref. [1] which we facilitate by inverting the temperatures from ref. [1] via Eq. 1 thereby obtaining the experimental isotope yield ratios. The resulting values and uncertainties for R_{HeLi} are listed in Table I and shown in Figure 1 by the horizontal cross-hatched areas. Temperatures extracted from the intersection of the cross-hatched areas and the calculations in each panel are indicated by the vertical cross-hatched regions; these ranges are also given in Table 1. Well defined lower (upper) limits to the temperature can only be established when the calculated values become higher (lower) than the measured ones at low (high) temperature.

Upper limits to the temperature are therefore not established for the data points at $E_o/A_o =$ 13.2 and 15.1 MeV, due to the insensitivity of the Helium-Lithium thermometer at $T_{em} > 7$ MeV for this system.

To understand this behavior, one can examine the predicted isotope yield ratios, $Y(^6Li)/\ Y(^7Li)$ and $Y(^3He)/\ Y(^4He)$, listed in Table I. Reflecting the small difference between the binding energies of the two Lithium isotopes, the $Y(^6Li)/\ Y(^7Li)$ ratio remains relatively constant around 1.0. In contrast, the $Y(^3He)/Y(^4He)$ ratio increases steadily with increasing temperature until around 7 MeV before flattening out. Thus, T_{HeLi} is essentially determined by the $Y(^3He)/Y(^4He)$ ratio. Consistent with Eq. 1, the calculated values for $Y(^3He)/Y(^4He)$ increase with temperature when secondary decay is neglected. However, when secondary decay is considered, the yield of ^4He is dramatically enhanced by the α decays of heavier particle unstable nuclei and the sensitivity of the ratio to temperature diminishes. Eventually, it becomes impossible to extract the upper limit for any temperatures greater than 7 MeV. These same conclusions will apply to any other isotope temperature involving the $Y(^3He)/Y(^4He)$ ratio.

In summary, sequential decay calculations which include both discrete states and unbound states in the continuum indicate that the secondary decay from continuum states strongly modifies temperatures derived from the Helium-Lithium double isotope ratio. Temperatures extracted by a reanalysis of the data of ref. [1] do not support claims for the observation of a strong rise in the temperature consistent with production of nuclear systems in a gaseous phase; the trends are similar to those extracted in previous analyses of excited state populations [27]. Strong secondary decay contributions to the calculated ^4He yields make the extraction of very high temperatures from the isotope ratios involving $Y(^3He)\ /Y(^4He)$ ratios problematic. These problems are likely to be compounded if there are significant non-thermal contributions to either the ^3He or ^4He yields as predicted by transport theory [28]. In this respect, it may be worthwhile to extend investigations to other thermometers involving only heavier isotopes.

REFERENCES

[1] J. Pochodzalla et al., Phys. Rev. Lett. **75**, 1040 (1995).

[2] D.H.E. Gross, Phys. Rev. Lett. **56**, 1544 (1986).

[3] J.P. Bondorf, R. Donangelo, I.N. Mishustin, C.J.Pethick, H. Schulz, K.Sneppen, Nucl. Phys. **A443** (1985) 321; Nucl. Phys. **A444** (1986) 460.

[4] M.B. Tsang et. al, Phys. Rev. C53, R1057.

[5] M.B. Tsang, W.G. Lynch, H. Xi, W.A. Friedman, MUSNSCL preprint 1035 (1996).

[6] A. Kolomeits et al., Phys. Rev. *C* (in press).

[7] X. Campi, H. Krivine, E. Plagnol, Phys. Rev. *C* (submitted)

[8] S. Albergo, S.Costa, E.Costanzo, A.Rubbino, Nuovo Cimento **89**, 1 (1985).

[9] Z. Majka, P.staszel, J.Cibor, J.B.Natowitz, K.Hagel, J.Li, N.Mdeiwayeh, R.wada and Y.Zhao, submitted to Phys. Rev. *C*.

[10] D. Hahn and H. Stocker, Nucl. Phys. **A476**, 718 (1988).

J. Konopka, H.Graf, H.Stoker, W.Griener, Phys. Rev. **C50**, 2085 (1994)

[11] A. Gilbert, A.G. W. Cameron, Canadian Journal of Physics, 43 (1965) 1446.

[12] T.K. Nayak et al., Phys. Rev. *C* 45, 132 (1992).

[13] H.M. Xu et. al., Phys. Rev. *C* 40, 186 (1989).

F. Zhu et al., Phys. Rev. *C* 52, 784 (1995).

[14] Z. Chen, C.K. Gelbke, Phys. Rev. **C38**, 2630 (1988).

[15] F. Ajzenberg-Selove, Nucl. Phys. **A392**, 1(1983); **A413**, 1 (1984); **A433**, 1 (1985); **A449**, 1 (1985); **A460**, 1 (1986).

[16] Previous investigations [4,12,14] have constrained calculations to describe the experi-

mental charge distributions by varying the Coulomb barrier.

[17] W. Hauser and H. Feshbach, Phys. Rev. **87**, 366 (1952).

[18] J. Randrup, S.E. Koonin, Nucl. Phys. **A356**, 223 (1981).

[19] W.A. Friedman and W.G. Lynch, Phys. Rev. **C28** (1983) 16; **C28** (1983) 950.

[20] M.G. Mustafa, M. Blann, A.V. Ignatyuk, S.M. Grimes., Phys. Rev. **C45**, 1078 (1992).

[21] V.F. Weisskopf, Phys. Rev. **52**, 295 (1937).

[22] H. Xi et al, to be published.

[23] C.A. Ogilvie et. al., Nucl. Phys. **A553**, 271c (1993).

[24] B.H. Sa, D.H.E. Gross, Nucl. Phys., **A437**, 643 (1985),

D.H.E. Gross, X.Z. Zhang, S.Y. Xu, Phys. Rev. Lett., **56**, 1544 (1986).

[25] J.P. Bondorf, R. Donangelo, I.N. Mishustin, H. Schulz, Nucl. Phys A444, 460 (1985).

[26] One could require the centroids of calculated and measured isotope distribution to agree instead of requiring the charge to mass ratio of emitted fragments to equal the initial charge to mass ratio, but such isotope information is not available for this reaction.

[27] C. Schwarz et. al. Phys. Rev. *C* 48, 676 (1993) and references therein.

[28] P. Danielewica, Phys. Rev. **C51**, 716 (1995).

FIGURES

FIG. 1. Dependence of the isotope yield ratios as a function of the emission temperatures, T_{em}, input to the sequential decay calculations. The horizontal hatched areas indicate the measured isotope yield ratios and the vertical shaded areas indicate the range of the extracted isotope temperatures.

TABLES

TABLE I. List of parameters [1, 23] used in sequential decay calculations.

$< E_o/A_o >$ (MeV)	2.2	4.1	5.6	9.9	11.6	13.2	15.1
Z_{Bound} [1]	75	64	55	35	25	15	5
τ [23]	3.1±0.3	2.4±0.3	2.2±0.3	1.8±0.3	1.9±0.3	2.5±0.3	4.5±0.7
A_o[1]	195	185	170	132	115	90	50
Z_o	80	76	70	54	47	37	21
R_{HeLi} [1]	10-30	14-25	11-19	8.1-11	5.0-5.8	3.9-5.0	2.5-2.9
T_{HeLi} (MeV) [1] C=1.2	4.6±0.6	4.4±0.3	4.8±0.2	5.3±0.2	6.5±0.2	7.2±0.3	9.0±0.5
T_{em} (MeV)	3.2-4.6	3.4-4.2	3.7-4.5	4.6-5.4	6.0-6.7	> 6.0	>7.2
$Y(^3He)/Y(^4He)$	0.05	0.05	0.075	0.085	0.15	>0.2	>0.2
$Y(^6Li)/Y(^7Li)$	0.8	0.8	0.8	0.8	0.9	1.0	1.2

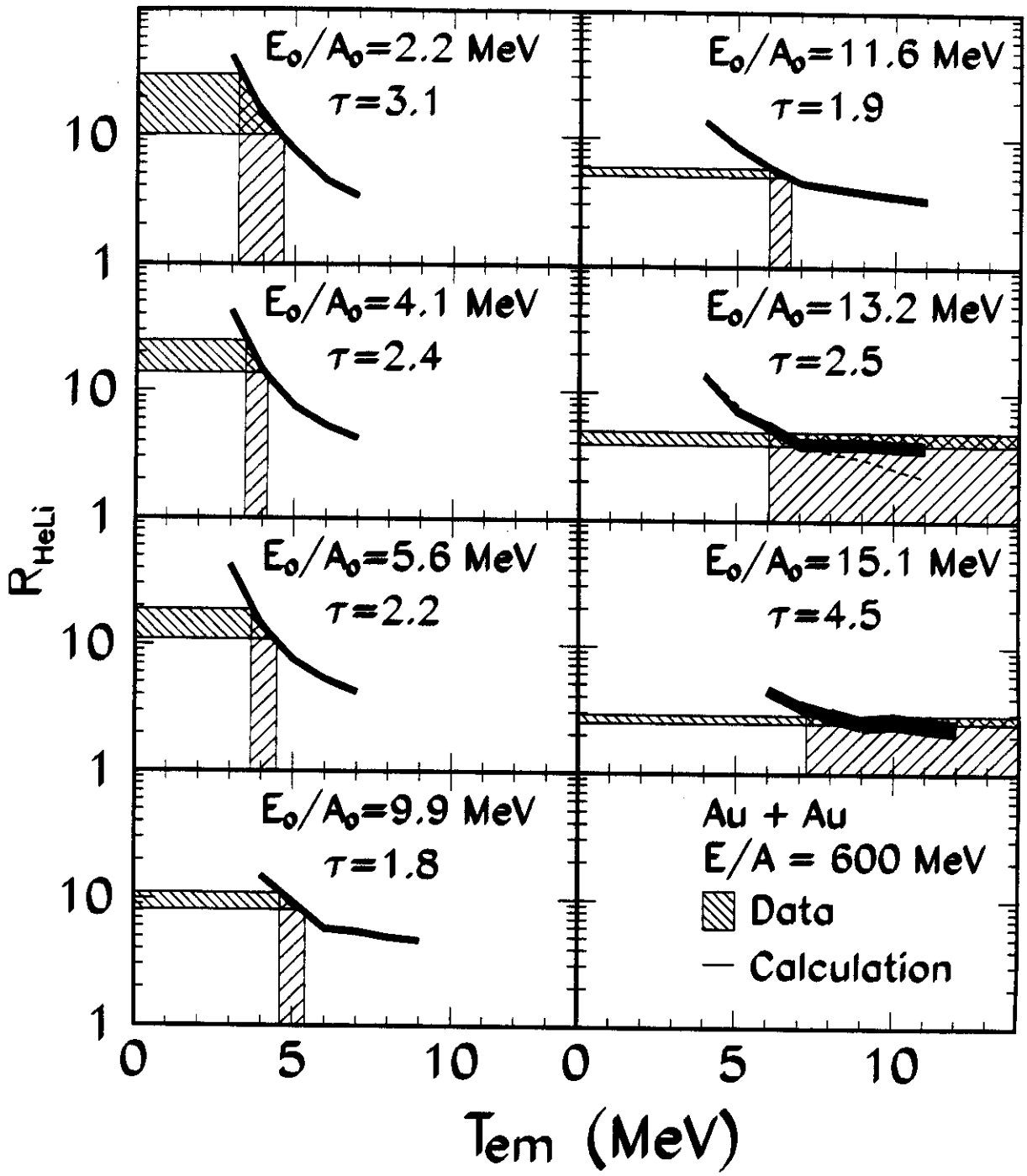
E_o/A_o=2.2 MeV
τ=3.1
E_o/A_o=11.6 MeV
τ=1.9
E_o/A_o=4.1 MeV
τ=2.4
E_o/A_o=13.2 MeV
τ=2.5
E_o/A_o=5.6 MeV
τ=2.2
E_o/A_o=15.1 MeV
τ=4.5
E_o/A_o=9.9 MeV
τ=1.8
Au + Au
E/A = 600 MeV
Data
Calculation
R_{HeLi}
10
1
0
5
10
T_{em} (MeV)